Homologous Series of Phenylquinoline-Carbazole Main Ligand Based On Red-Emitting Iridium(III) Complexes for Phosphorescent Organic Light-Emitting Diodes

ARTICLE *in* THE JOURNAL OF PHYSICAL CHEMISTRY C · MARCH 2012

Impact Factor: 4.77 · DOI: 10.1021/jp2101094

7 AUTHORS, INCLUDING:

Myungkwan Song
Korea Institute of Materials Science
97 PUBLICATIONS **930** CITATIONS
SEE PROFILE

Sunwoo Kang
Samsung Display, South Korea
54 PUBLICATIONS **939** CITATIONS
SEE PROFILE

THE JOURNAL OF PHYSICAL CHEMISTRY C

Article

pubs.acs.org/JPCC

Homologous Series of Phenylquinoline-Carbazole Main Ligand Based On Red-Emitting Iridium(III) Complexes for Phosphorescent Organic Light-Emitting Diodes

Myungkwan Song,[†] Jin Su Park,[†] Yeong-Soon Gal,[‡] Sunwoo Kang,[§] Jin Yong Lee,[§] Jae Wook Lee,*[,∥] and Sung-Ho Jin*[,†]

[†]Department of Chemistry Education, Interdisciplinary Program of Advanced Information and Display Materials, and Institute for Plastic Information and Energy Materials, Pusan National University, Busan 609-735, Republic of Korea

[‡]Polymer Chemistry Laboratory, Kyungil University, Hayang 712-701, Republic of Korea

[§]Department of Chemistry, Sungkyunkwan University, Suwon 440-746, Republic of Korea

[∥]Department of Chemistry, Dong-A University, Busan 604-714, Republic of Korea

ABSTRACT: New red-emitting phosphorescent Ir(III) complexes, bis[9-ethyl-2-(4-phenylquinolin-2-yl)-9*H*-carbazolato-N,$C^{2'}$]iridium picolinate-*N*-oxide [(2-Et-CVz-PhQ)$_2$Ir(pic-N-O)] and bis[9-ethyl-3-(4-phenylquinolin-2-yl)-9*H*-carbazolato-N,$C^{2'}$]iridium picolinate-*N*-oxide (3-Et-CVz-PhQ)$_2$Ir(pic-N-O), were synthesized, and their applications in phosphorescent organic light-emitting diodes (PhOLEDs) as well as their photophysical, electrochemical, and electroluminescent (EL) properties were investigated. To tune the performance of PhOLEDs containing these substances, the 9-ethyl-2-(4-phenylquinolin-2-yl)-9*H*-carbazole (2-Et-CVz-PhQ) and 9-ethyl-3-(4-phenylquinolin-2-yl)-9*H*-carbazole (3-Et-CVz-PhQ) were prepared and used as main ligands for the synthesis of Ir(III) complexes. The solution processed red PhOLEDs with a configuration of ITO/PEDOT:PSS/TCTA/PVK or 3-Et-CVz-PhQ:TPD:OXD-7:Ir complex/cathode were fabricated. The maximum EL emission peaks of (2-Et-CVz-PhQ)$_2$Ir(pic-N-O) and (3-Et-CVz-PhQ)$_2$Ir(pic-N-O) were observed at 689 and 609 nm, respectively. The PhOLEDs with (2-Et-CVz-PhQ)$_2$Ir(pic-N-O) and (3-Et-CVz-PhQ)$_2$Ir(pic-N-O) exhibited respective maximum external quantum efficiencies of 4.32% and 8.74% along with CIE (Commission International de l'Eclairage) coordinates of (0.68, 0.28) and (0.62, 0.37), respectively. Furthermore, by introducing a TCTA interlayer, the PhOLEDs showed a slight efficiency roll off of 15% from a low current density (1 mA/cm^2) to a high current density (30 mA/cm^2). The electro-optical properties and the performance of PhOLEDs, prepared by using the two Ir(III) complexes, were probed through the use of density functional theory (DFT) calculations.

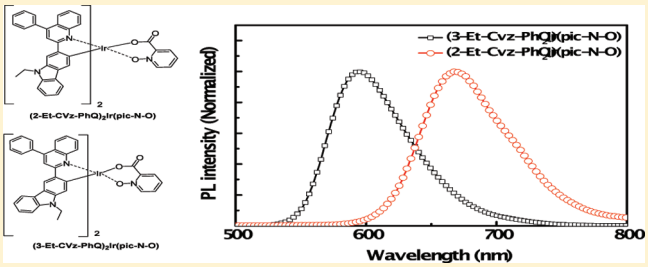

INTRODUCTION

Organic light-emitting diodes (OLEDs) have received great attention due to their potential applications in full-color flat panel displays and solid-state lighting.[1] Internal quantum efficiencies near unity, corresponding to the harvesting of all singlet and triplet states, can be achieved in OLEDs composed of phosphorescent complexes based on ligated iridium (Ir), platinum, ruthenium, and osmium.[2,3] Among these phosphorescent emitters, Ir(III) complexes have been shown to give the best performance. Because of their relatively short triplet lifetimes, potential high device efficiencies, and emission wavelength tunability from blue to deep-red, Ir(III) complexes have received particular attention as efficient dopants for applications in the area of phosphorescent OLEDs (PhOLEDs).[4] The efficiencies, brightness, and wavelength emissions of Ir(III) complexes strongly depend on the molecular structure of a cyclometalated ligand. The emission wavelength of Ir(III) complexes normally can be altered by changing the electron density or position of substituents on the main ligands. For example, emission wavelengths of these Ir(III) complexes can be adjusted to cover the entire visible spectral region by modifying or varying cyclometalated 2-arylpyridine ligands.[5] Therefore, the design and preparation of novel cyclometalated ligands for Ir(III) complexes has attracted great attention.[6]

In most applications, PhOLEDs have been prepared by using thermal evaporation of up to six organic layers.[7,8] This protocol makes the fabrication process relatively complicated and expensive due to the waste of 90% of materials. The solution processing technology will be an alternative solution for PhOLEDs fabrication because of scalability and cost competitiveness by simple device structure. The majority of PhOLEDs composed of solution-processed layers contain oligomers or conjugated polymers,[9,10] and more recently dendrimers.[11,12] One of the disadvantages associated with the

Received: October 21, 2011
Revised: January 24, 2012
Published: March 9, 2012

use of these types of materials is the difficulty in obtaining highly purified products. Carbazoles (CVz) exhibit an inherent electron-donating ability, excellent photoconductivity, and relatively intense luminescence.[13,14] Moreover, the 3/6 or 2/7 positions of carbazole group can be readily functionalized and covalently linked to other molecular units, thus enabling the optimization of processability of the resulting materials. In recent years, there have been some reports about PhOLEDs using a 3/6 or 2/7 position of carbazole-based Ir(III) complexes as the emitting material. XZhang et al. reported red PhOLEDs using PVK host with a maximum luminance of 6402 cd/m^2 at 24.8 V and a maximum luminance efficiency of 5.56 cd/A.[15] Yang et al. obtained a red PhOLEDs with efficiencies of 12.18 cd/A and 4.63 lm/W at 15.3 V with CIE coordinates of (0.63, 0.37).[16] In these cases, the red PhOLEDs are fabricated by vacuum deposition method, which requires a relatively complex technological process and brings about a large amount of wasted organic materials, resulting in relatively high fabrication costs.

Despite their significant biological activities, phenylquinoline (PhQ) derivatives have been explored in the context of formation of conjugated molecules and polymers that combine enhanced electronic, optoelectronic, or nonlinear optical properties, along with excellent mechanical characteristics.[17,18] By using the synergistic properties of CVz and PhQ, we recently designed and prepared novel main ligands for Ir(III) complexes, which are comprised of PhQ units linked to the C-3 position of CVz (3-Et-CVz-PhQ), for use in deep-blue OLEDs.[19] In addition, we described a new family of red Ir(III) complexes that are based on a 3-Et-CVz-PhQ main ligand and a picolinic acid N-oxide (pic-N-O) ancillary ligand, and we showed that they can be employed for high efficiency solution processing of red PhOLEDs.[20]

We anticipated that ligation of Ir(III) with the C-2 and C-3 positions of CVz moieties in Et-CVz-PhQ would result in the creation of different band gaps in a tunable manner. In particular, there has not been any report to date using Ir(III) by ligation with C-2 or C-3 position of CVz in Et-CVz-PhQ main ligand. Another advantage of Ir(III) complexes that incorporate Et-CVz-PhQ as the main ligand is high organic solvent solubility, improved charge balance in the electroluminescent (EL) process, and enhanced thermal stability. Below, we outline the results of studies aimed at exploring these proposals. In this effort, we synthesized novel Ir(III) complexes, (2-Et-CVz-PhQ)$_2$Ir(pic-N-O), which contain Ir(III) ligated at the C-3 position of a CVz segment in the 2-Et-CVz-PhQ main ligand. In addition, we have probed the redox, photophysical, and EL properties of these new red-emitting heteroleptic Ir(III) complexes.

EXPERIMENTAL SECTION

General Information. Unless otherwise specified, all reactions were carried out under a N_2 atmosphere using standard Schlenk techniques. Solvents were dried and purified by fractional distillation over sodium/benzophenone and handled in a moisture-free atmosphere. Column chromatography was performed using silica gel (Merck, 250−430 mesh). ^{1}H and ^{13}C NMR spectra were recorded using a Bruker AM-300 spectrometer, and the chemical shifts were recorded in ppm relative to internal standards. Thermal analyses were carried out on a Mettler Toledo TGA/SDTA 851e, DSC 822e analyzer under a N_2 atmosphere at a heating rate of 10 °C/min. Cyclic voltammetry (CV) was carried out with a CHI 600C potentiostat (CH Instruments) at a scan rate of 100 mV/s in a 0.1 M solution of tetra-*n*-butylammonium hexafluorophosphate ($TBAPF_6$) in anhydrous acetonitrile/benzene (1:1.5 v/v). A platinum wire was used as the counter electrode, and an Ag/$AgNO_3$ was used as the reference electrode. All electrochemical experiments were performed under an Ar atmosphere at room temperature. The absorption and photoluminescent (PL) spectra were measured by using a Jasco V-570 UV−visible spectrometer and a Hitachi F-4500 fluorescence spectrophotometer, respectively.

Synthesis of 9-Ethyl-2-(4-phenylquinolin-2-yl)-9*H*-carbazole (2-Et-CVz-PhQ). A mixture of the 2-acetyl-*N*-ethylcarbazole (1 g, 4.2 mmol), 2-aminobenzophenone (0.91 g, 4.6 mmol), diphenyl phosphate (DPP, 1.27 g, 5.1 mmol), and *m*-cresol (5.0 mL) was flushed with N_2 while stirring at room temperature for 20 min and then stirred at 140 °C for 12 h. Addition to 10% triethylamine/ethanol resulted in the formation of a precipitate, which was collected by using vacuum filtration. The filtrate was eluted through silica gel and concentrated in vacuo giving a solid, which was then recrystallized twice from a chloroform/hexane to give 2-Et-CVz-PhQ (84%) as yellowish crystals. ^{1}H NMR (300 MHz, $CDCl_3$, δ): 1.49−1.54 (t, 3H), 4.50−4.52 (q, J = 7.14 Hz, 2H), 7.25−7.65 (m, 11H), 8.00−8.18 (m, 3H), 8.23−8.34 (m, 2H), 8.37 (s, 1H). ^{13}C NMR (300 MHz, $CDCl_3$, δ): 156.7, 150.6, 147.4, 146.3, 137.9, 136.5, 131.7, 129.9, 129.3, 128.9, 128.3, 127.4, 127.0, 125.1, 122.2, 120.1, 119.4, 118.9, 118.7, 111.1, 109.6, 106.2, 102.4, 48.2, 15.7. Anal. Calcd for $C_{29}H_{22}N_2$: C, 87.41; H, 5.56; N, 7.03. Found: C, 87.08; H, 5.58; N, 7.05.

Synthesis of (2-Et-CVz-PhQ)$_2$Ir(pic-N-O). The cyclometalated Ir(III) μ-chloride bridged dimer $[(\hat{C}N)_2Ir(\mu\text{-}Cl)]_2$ was synthesized by using the method reported by Nonoyama.[21] 9-Ethyl-2-(4-phenylquinolin-2-yl)-9*H*-carbazole (2-Et-CVz-PhQ) (1.5 g, 3.76 mmol) and $IrCl_3{\cdot}H_2O$ (0.60 g, 1.71 mmol) were added to a mixture of 2-ethoxyethanol and water (100 mL, 3:1 v/v). The mixture was stirred at 140 °C for 20 h, and a brown precipitate was obtained after cooling to room temperature. The precipitate was collected and washed sequentially with deionized water (80 mL) and methanol (40 mL). Subsequently, the cyclometalated Ir(III) μ-chloride bridged dimer was dried under vacuum to afford a brown solid. Cyclometalated Ir(III) μ-chloride bridged dimer (0.5 g, 0.24 mmol) and pic-N-O (0.18 g, 1.22 mmol) were mixed with Na_2CO_3 (0.26 g, 2.45 mmol) in 2-ethoxyethanol (30 mL). The mixture was stirred at reflux for 12 h under a N_2 atmosphere, cooled to room temperature, and poured into water. The aqueous solution was extracted with ethyl acetate, and the extracts were dried over anhydrous $MgSO_4$ and concentrated in vacuo. The residue was subjected to silica gel chromatography (hexane:ethyl acetate = 1:4), and the solid obtained was recrystallized twice using dichloromethane/hexane to afford (2-Et-CVz-PhQ)$_2$Ir(pic-N-O) as a red solid complex (0.2 g, 75%). ^{1}H NMR (300 MHz, $CDCl_3$): δ (ppm) 8.88 (d, J = 8.7 Hz, 1H), 8.25 (d, 2H), 8.07 (s, 1H), 8.01 (d, 1H), 7.95 (s, 1H), 7.86 (d, J = 7.5 Hz, 1H), 7.78−7.55 (m, 15H), 7.45−7.13 (m, 9H), 7.02 (s, 1H), 6.93−6.83 (m, 3H), 6.77 (t, 1H), 4.43−4.33 (m, 4H), 1.53 (t, J = 7.2 Hz, 3H), 1.41 (t, J = 7.2 Hz, 3H). ^{13}C NMR (300 MHz, $CDCl_3$): δ (ppm) 172.1, 170.7, 168.9, 153.0, 150.4, 150.3, 149.1, 148.2, 146.4, 144.4, 143.3, 141.6, 141.2, 140.9, 137.9, 137.8, 137.4, 137.2, 136.8, 136.2, 131.6, 129.8, 129.1, 128.9, 128.8, 128.7, 128.2, 127.4, 127.0, 126.7, 126.5, 126.4, 126.2, 125.9, 125.8, 125.7, 125.6, 125.5, 125.3, 121.9, 121.6, 121.3, 120.8, 118.2, 118.1, 117.6, 116.9, 108.0, 106.7,

dx.doi.org/10.1021/jp2101094 | J. Phys. Chem. C 2012, 116, 7526−7533

Scheme 1. Synthetic Sequences for the Preparation of the (2-Et-CVz-PhQ)$_2$Ir(pic-N-O) and Molecular Structure of (3-Et-CVz-PhQ)$_2$Ir(pic-N-O)

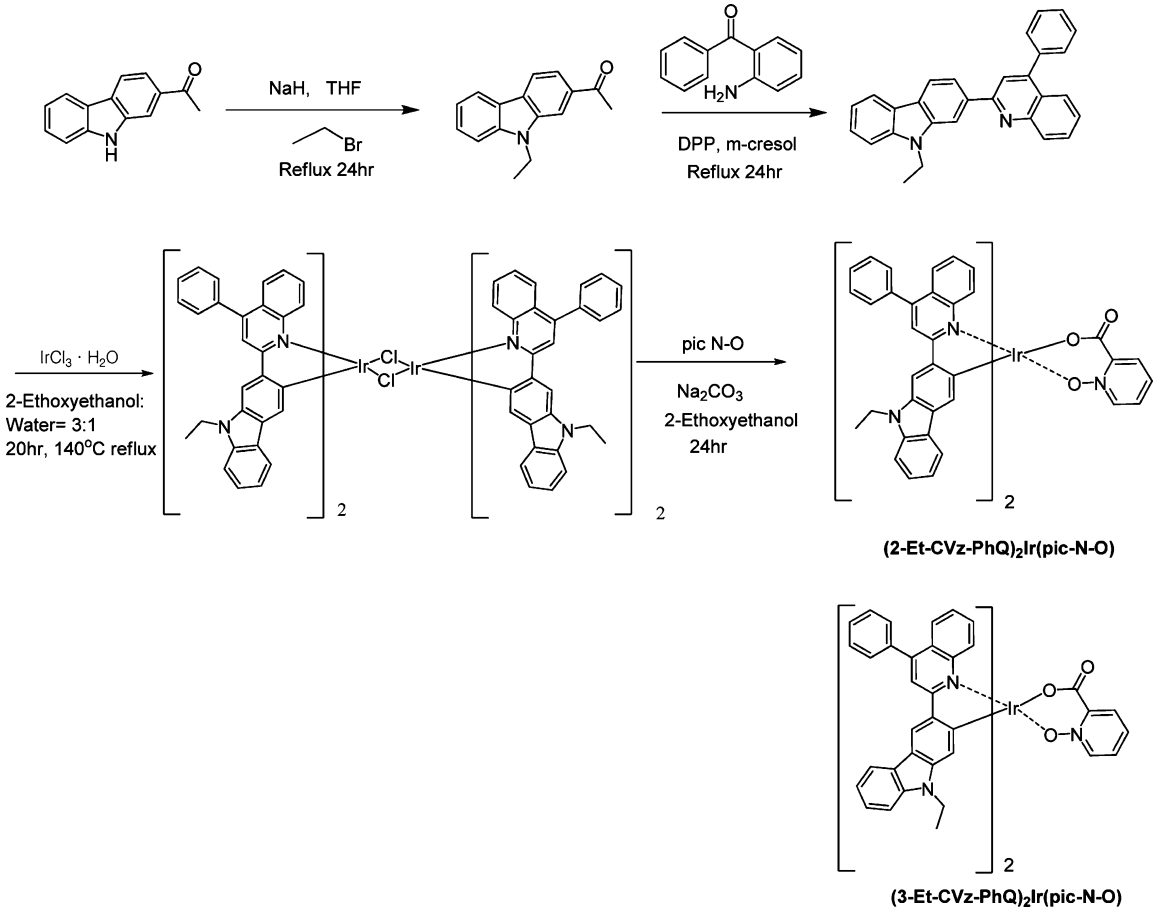

106.5, 37.4, 37.2, 14.0, 13.9. Anal. Calcd for $C_{64}H_{46}N_5O_3Ir$: C, 68.31; H,4.12; N, 6.22. Found: C, 68.51; H, 4.11; N, 6.20. MS(TOF): m/z = 1125 [M^+] calcd for $C_{64}H_{46}IrN_5O_3$, 1125.

PhOLED Fabrication and Measurements. Indium tin oxide (ITO) glass substrates with a sheet resistance of 20 Ω per square were washed sequentially with a substrate-cleaning detergent, deionized water, acetone, and isopropyl alcohol, and finally treated with UV-ozone chamber for 15 min. The layer of PEDOT:PSS (40 nm, CLEVIOS P VP AI 4083) was spin-coated onto the precleaned and UV-ozone treated ITO substrates. Next, the spin-coated film was baked in air at 150 °C for 20 min. Subsequently, the interlayer solution of TCTA (0.5 wt %, toluene, 30 nm) was spin coated and followed by drying at 180 °C for 30 min on a hot plate. The emitting layer was then spin-coated onto the interlayer coated substrate from a solution of PVK (or 3-Et-CVz-PhQ), OXD-7, TPD, and (3-Et-CVz-PhQ)$_2$Ir(pic-N-O) or (2-Et-CVz-PhQ)$_2$Ir(pic-N-O) in chlorobenzene. All solutions used in PhOLED fabrications were filtered through a 0.20 μm PTFE (hydrophobic) syringe filter. The film was then baked at 80 °C for 30 min in a glovebox. In all cases, doping concentrations of the (3-Et-CVz-PhQ)$_2$Ir(pic-N-O) or (2-Et-CVz-PhQ)$_2$Ir(pic-N-O) were fixed at 6 wt %. A typical cathode, consisting of OXD-7 (20 nm)/Ba (3 nm)/Al (100 nm), was thermal vapor deposited with an effective area of 4 mm^2 at a pressure 5 × 10^{-6} Torr. The film thickness was measured using an α-Step IQ surface profiler (KLA Tencor, San Jose, CA). Two kinds of host devices were prepared to investigate the effect of host material properties on device performances. Devices I and II consist of a (3-CVz-PhQ)$_2$Ir-(pic-N-O) as an emitter and host of PVK and 3-Et-CVz-PhQ, respectively, and devices III and IV consist of (2-CVz-PhQ)$_2$Ir(pic-N-O) as an emitter and host of PVK and 3-Et-CVz-PhQ, respectively. EL spectra and current density−voltage−luminance (J−V−L) characteristics of the PhOLEDs were measured using a programmable Keithley model 236 power source and spectrascan CS-1000 photometer. All measurements were carried out in ambient atmosphere without further encapsulation.

Calculation Methods. Density functional theory (DFT) calculations were performed with 6-31G* basis sets for (3-Et-CVz-PhQ)$_2$Ir(picN-O) and (2-Et-CVz-PhQ)$_2$Ir(picN-O) employing the Becke's three parametrized Lee−Yang−Parr exchange functional (B3LYP) using a suite of Gaussian 03 programs.

RESULTS AND DISCUSSION

As stated above, the electro-optical properties and device performances of PhOLEDs, based on emission from Ir(III) complexes, can be altered by modifying the chemical structure and electronic characteristics of the main ligand. We proposed that the use of 9-ethyl-2-(4-phenylquinolin-2-yl)-9H-carbazole (2-Et-CVz-PhQ) and 9-ethyl-3-(4-phenylquinolin-2-yl)-9H-carbazole (3-Et-CVz-PhQ) as main ligands for Ir(III) complexes would manage in highest occupied molecular orbital (HOMO) and lowest unoccupied molecular orbital (LUMO) energies to improve charge balance and thus overall of PhOLED

dx.doi.org/10.1021/jp2101094 | J. Phys. Chem. C 2012, 116, 7526−7533

performance. These ligands were synthesized by using acid-catalyzed Friedlander condensation reactions.[22] Condensation reactions of either 2-acetyl-*N*-ethylcarbazole or 3-acetyl-*N*-ethylcarbazole with 2-aminobenzophenone gave the desired donor−acceptor type main ligands. The $(2\text{-Et-CVz-PhQ})_2$Ir(pic-N-O) complex was prepared by the procedure shown in Scheme 1. The cyclometalated Ir(III) μ-chloride bridged dimer, synthesized by addition of $IrCl_3 \cdot H_2O$ to an excess of 2-Et-CVz-PhQ according to the method by Nonoyama,[21] can be easily converted to a mononuclear Ir(III) complex $(2\text{-Et-CVz-PhQ})_2$Ir(pic-N-O) by replacing the two bridging chlorides with the bidentate monoanionic ancillary ligand (Scheme 1). The synthesis of $(3\text{-Et-Cvz-PhQ})_2$Ir(pic-N-O) was described in our previous report.[20] The Ir(III) complexes, obtained in the manner described above, were purified by using silica gel column chromatography followed by recrystallization and fully characterized by utilizing ^{1}H NMR, ^{13}C NMR, and elemental analyses.

The thermal properties of the new Ir(III) complexes were determined by employing TGA and DSC under a N_2 atmosphere at a heating rate of 10 °C/min. The results are given in Figure 1 and Table 1. The TGA curves indicate that

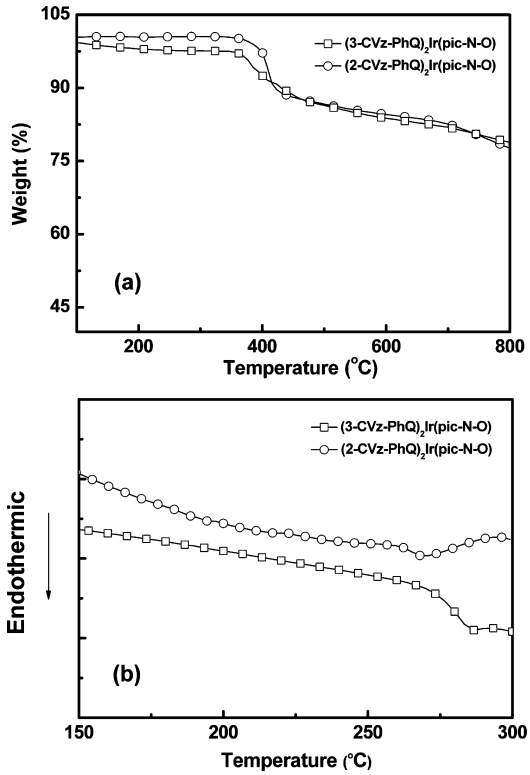

Figure 1. (a) TGA and (b) DSC data of $(3\text{-Et-CVz-PhQ})_2$Ir(pic-N-O) and $(2\text{-Et-CVz-PhQ})_2$Ir(pic-N-O) measured at a scan rate of 10 °C/min under N_2.

$(2\text{-Et-CVz-PhQ})_2$Ir(pic-N-O) and $(3\text{-Et-CVz-PhQ})_2$Ir(pic-N-O) lose less than 5% of their weight on heating at ca. 407 and 381 °C, respectively. The respective glass transition temperatures (T_g) of $(2\text{-Et-CVz-PhQ})_2$Ir(pic-N-O) and $(3\text{-Et-CVz-PhQ})_2$Ir(pic-N-O) were found to be 280 and 287 °C. The observations made in this investigation demonstrate that the Ir(III) complexes have excellent thermal stabilities, which indicates that they will not readily decompose under the high temperature conditions present during operation of PhOLEDs.

Interesting results have come from an investigation of the optical properties of the main ligands, which show that they are altered by a slight modification of the molecular structure. The UV−visible absorption and photoluminescent (PL) spectra of Ir(III) complexes in chloroform solutions at room temperature are shown in Figure 2, and these results are summarized in Table 1. The absorption spectra show broad bands in the 300−650 nm region and intense peaks at wavelengths below 400 nm, the latter of which are assigned to spin-allowed $\pi-\pi^*$ transitions. The bands extending into the visible region above 400 nm are assigned to spin-allowed metal−ligand charge transfer (^{1}MLCT) transitions, and the maxima observed at longer wavelengths are associated with spin−orbit coupling enhanced $^3\pi-\pi^*$ and ^{3}MLCT transitions.[23] The $(2\text{-Et-CVz-PhQ})_2$Ir(pic-N-O) complex exhibits a significantly longer wavelength absorption (extending to 650 nm) than that of $(3\text{-Et-CVz-PhQ})_2$Ir(pic-N-O) (extending to 550 nm). PL spectra of $(2\text{-Et-CVz-PhQ})_2$Ir(pic-N-O) and $(3\text{-Et-CVz-PhQ})_2$Ir(pic-N-O) contain emission peaks at 668 and 595 nm, respectively (Figure 2b). Thus, by slightly modifying the molecular structure of the Et-CVz-PhQ-based main ligand, the emission peak of the Ir(III) complex is red-shifted by 73 nm. This remarkable difference in emission wavelength is consistent with the difference observed in the ^{3}MLCT absorptions of the Ir(III) complexes, suggesting that emission is associated with triplet excited-state phosphorescent.[24] The phosphorescent quantum yields (Φ_{pl}) of Ir(III) complexes in chloroform solution and film state were measured with bis[2-(2′-benzothienyl)-pyridinato-N,C3′]iridium (acetylacetonate) $(piq)_2$Ir(acac) as a known red dopant (0.20).[25] The phosphorescent quantum yields for solution state of $(2\text{-Et-CVz-PhQ})_2$Ir(pic-N-O) and $(3\text{-Et-CVz-PhQ})_2$Ir(pic-N-O) were 0.06 and 0.20, respectively. Also, the Φ_{pl} values for film state of $(2\text{-Et-CVz-PhQ})_2$Ir(pic-N-O) and $(3\text{-Et-CVz-PhQ})_2$Ir(pic-N-O) were 0.03 and 0.16, respectively.

To investigate the charge carrier injection properties of the Ir(III) complexes, HOMO and LUMO energy levels were determined by carrying out redox measurements using cyclic voltammetry (CV). As shown in Figure 3, the Ir(III) complexes undergo reversible redox processes, suggesting that they are capable of stabilizing both the cation and anion radical states generated in PhOLEDs. On the basis of the onset potentials for oxidation and reduction, the respective HOMO and LUMO energy levels were determined to be −4.91 and −2.70 eV for $(2\text{-Et-CVz-PhQ})_2$Ir(pic-N-O) and −5.14 and −2.62 eV for $(3\text{-Et-CVz-PhQ})_2$Ir(pic-N-O). The results show that ligation of Ir(III) complex to the more electron-donating C3-position of the CVz moiety in the Et-CVz-PhQ-based main ligand results in an increase of the energy of the metal d orbital, which leads to a higher HOMO energy for $(2\text{-Et-CVz-PhQ})_2$Ir(pic-N-O). In contrast, ligation of the Ir(III) complex to the less electron-donating C2-position of the CVz group in $(3\text{-Et-CVz-PhQ})_2$Ir(pic-N-O) causes a smaller perturbation of the d orbital energy. Therefore, $(2\text{-Et-CVz-PhQ})_2$Ir(pic-N-O) has a smaller band gap than that of $(3\text{-Et-CVz-PhQ})_2$Ir(pic-N-O).

To illustrate the EL properties of the Ir(III) complexes, solution-processed PhOLEDs were fabricated with the following four configurations (Figure 4): devices I, II, ITO/PEDOT:PSS (40 nm)/TCTA (30 nm)/host:OXD-7:TPD:$(3\text{-Et-CVz-PhQ})_2$Ir(pic-N-O) (70 nm)/OXD-7 (20 nm)/Ba (3 nm)/Al (100 nm); devices III, IV, ITO/PEDOT:PSS (40 nm)/TCTA (30 nm)/host:OXD-7:TPD:$(2\text{-Et-CVz-PhQ})_2$Ir(pic-N-O) (70 nm)/OXD-7 (20 nm)/Ba (3 nm)/Al (100 nm), using

dx.doi.org/10.1021/jp2101094 | J. Phys. Chem. C 2012, 116, 7526−7533

Table 1. Photophysical, Electrochemical, and Thermal Data for the Red-Emitting Ir(III) Complexes

compound	T_d (°C)[a]	T_g (°C)[b]	λ_{abs} (log ε (nm))[c]	λ_{em} (nm)[d]	Φ_{pl} (%)[e]	Φ_{pl} (%)[f]	τ_p (μs)[g]	HOMO/LUMO (eV)[h]
(3-Et-CVz-PhQ)$_2$Ir(pic-N-O)	381	287	318(5.2), 353(5.0), 375(5.0), 404(4.8), 479(4.1)	595	0.20	0.16	3.72	−5.14/−2.62
(2-Et-CVz-PhQ)$_2$Ir(pic-N-O)	407	280	317(5.0), 338(5.0), 378(5.1), 558(4.0)	668	0.06	0.03	3.69	−4.91/−2.70

[a]Temperature with 5% mass loss measure by TGA with a heating rate of 10 °C/min under N_2. [b]Glass transition temperature, determined by DSC with a heating rate of 10 °C/min under N_2. [c]Measured in $CHCl_3$ solution. [d]Maximum emission wavelength, measured in $CHCl_3$ solution. [e]Measured in 1×10^{-5} M degassed $CHCl_3$ solution relative to Ir(piq)$_2$(acac) (Φ_{pl} = 0.20) with 450 nm excitation. [f]Measured in film state relative to Ir(piq)$_2$(acac) (Φ_{pl} = 0.20) with 450 nm excitation. [g]Emission decay time measured after 4 ns pulsed excitation at λ = 337 nm. [h]Determined from the onset of oxidation and reduction potentials.

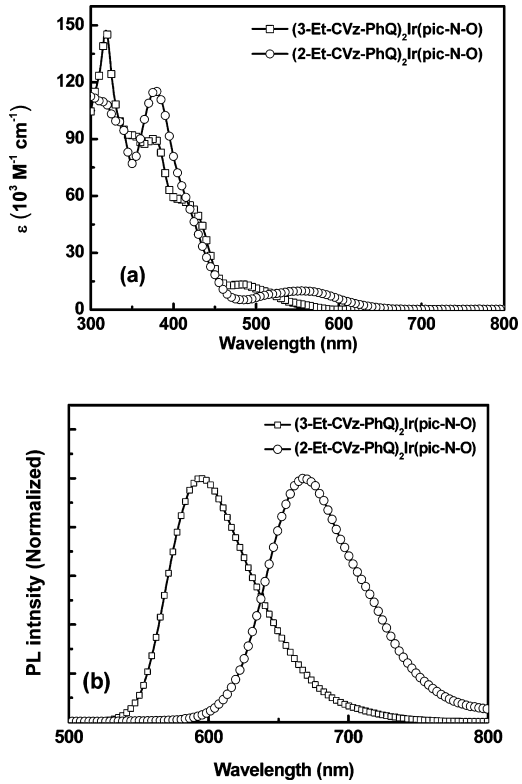

Figure 2. (a) UV−visible absorption and (b) PL spectra of (3-Et-CVz-PhQ)$_2$Ir(pic-N-O) and (2-Et-CVz-PhQ)$_2$Ir(pic-N-O) in $CHCl_3$ at 25 °C.

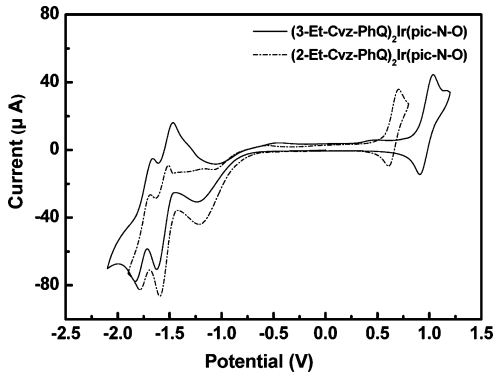

Figure 3. CV of (3-Et-CVz-PhQ)$_2$Ir(pic-N-O) and (2-Et-CVz-PhQ)$_2$Ir(pic-N-O) in tetra-*n*-butylammonium hexafluorophosphate ($TBAPF_6$) at a scan rate of 100 mV/s.

(2-Et-CVz-PhQ)$_2$Ir(pic-N-O) or (3-Et-CVz-PhQ)$_2$Ir(pic-N-O) as a dopant material and PVK:TPD:OXD-7 (3:1:1) (device I and III) or 3-Et-CVz-PhQ:TPD:OXD-7 (3:1:1) (device II and IV) as a host system. Standard devices with host of PVK and 3-Et-CVz-PhQ (devices V and VI) using (btp)$_2$Ir(acac) red dopant were fabricated as reference devices.

3-Et-CVz-PhQ was found to exhibit excellent host properties in deep-blue OLEDs[19] and to have good film-forming properties of the emitting layer as a result of the molecular similarity between 3-Et-CVz-PhQ and two Ir(III) complexes. In these devices, 4,4′,4″-tri(*N*-carbazoyl)triphenylamine (TCTA) was used as the hole injection/transporting and exciton blocking material, and *N*,*N*′-diphenyl-*N*,*N*′-bis(3-methylphenyl)-(1,1′-biphenyl)-4,4′-diamine (TPD) and 1,3-bis[(*p*-tert-butyl)phenyl-1,3,4-oxadiazoyl]benzene (OXD-7) were utilized as the hole transporting and hole blocks/electron transporting materials.

Figure 4 shows the energy band diagrams of the materials used in the fabricated PhOLEDs. The HOMO and LUMO energies of the Ir(III) complexes lie above and below those of the PVK host. The HOMO energy level of 3-Et-CVz-PhQ is lower than those of Ir(III) complexes. However, the energy of the LUMO of 3-Et-CVz-PhQ is slightly higher than or similar to that of the Ir(III) complexes. From viewing these energy band diagrams, it can be seen that the Ir(III) complexes will trap both electrons and holes within their emitting layers. Moreover, the hole blocking/electron transporting layer (OXD-7) serves to effectively enable electron injection/transport and charge carrier balance within the emitting layer. The LUMO energy of OXD-7 is close to that of the Ir(III) complexes in the emitting layer, an important feature that ensures efficient electron injection into both the transport molecules and the Ir(III) complexes.

EL spectra of the Ir(III) complexes in solution-processed PhOLEDs are displayed in Figure 5. The maximum emission peaks of (2-Et-CVz-PhQ)$_2$Ir(pic-N-O) and (3-Et-CVz-PhQ)$_2$Ir(pic-N-O) are observed at 689 and 609 nm, respectively. On the other hand, the maximum emission peak of (btp)$_2$Ir(acac) showed at 617 nm, with a shoulder peak at 671 nm, respectively. Because of the shift of the exciton recombination zones, the EL spectra of the PhOLEDs display a greater red shift than those seen in the PL spectra. The fact that no emission originates from TPD and OXD-7 indicates that these substances function as effective blockers to confine carriers and excitons to the emitting layer. The EL spectra of the different host systems are almost identical, showing again that emission takes place mainly from the triplet states of the Ir(III) complexes and not from TPD and OXD-7. This observation demonstrates that charge trapping rather than energy transfer is the predominant mechanism of EL in these PhOLEDs.

dx.doi.org/10.1021/jp2101094 | J. Phys. Chem. C 2012, 116, 7526−7533

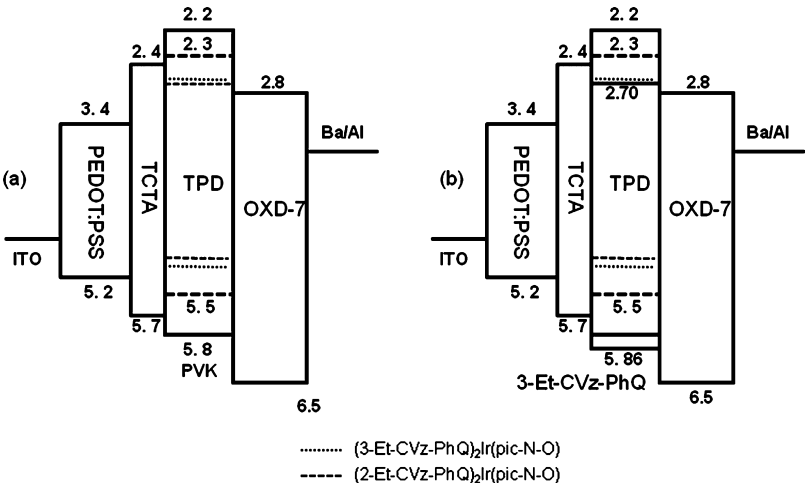

Figure 4. Configuration and energy level diagrams for the materials used for the preparation of the PhOLEDs using PVK (a) and 3-Et-CVz-PhQ (b) as host materials.

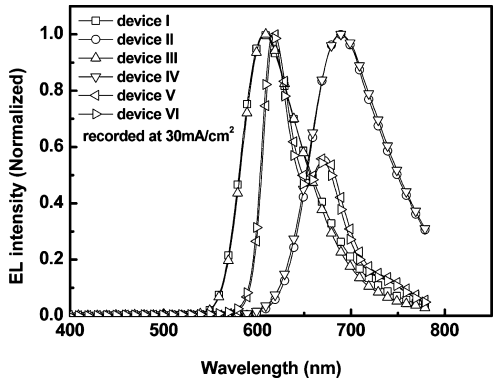

Figure 5. Electroluminescence (EL) spectra of devices I–IV.

The current density–voltage–luminance (J–V–L) characteristics of solution-processed PhOLEDs, fabricated using (3-Et-CVz-PhQ)$_2$Ir(picN-O), (2-Et-CVz-PhQ)$_2$Ir(picN-O), and (btp)$_2$Ir(acac) as dopants and PVK:TPD:OXD-7 and 3-Et-CVz-PhQ:TPD:OXD-7 as host systems, are displayed in Figure 6. The performances and EL emission characteristics of the PhOLEDs are summarized in Table 2. PhOLEDs containing the Ir(III) complexes have turn-on voltages in the range of 6–6.5 V. The slight difference between the turn-on voltages of the PhOLEDs can be attributed to differences in the thickness of the spin-coated emission layers. The performances of solution-processed PhOLEDs, composed of PVK:TPD:OXD-7, are relatively high as compared to those comprised of the 3-Et-CVz-PhQ:TPD:OXD-7 host system. As reported by Neher et al., the low efficiency of the 3-Et-CVz-PhQ:TPD:OXD-7 host may be a consequence of a significant quenching effect exerted by 3-Et-CVz-PhQ blended in the emissive layer that serves as an energy trap.[26] 3-Et-CVz-PhQ has a nonemissive triplet state, which lies at a lower energy as compared to (3-Et-CVz-PhQ)$_2$Ir(picN-O) and (2-Et-CVz-PhQ)$_2$Ir(picN-O). This phenomenon might lead to efficient triplet harvesting. From inspection of the J–V characteristics, it can be seen that PhOLEDs with PVK:TPD:OXD-7 as a host show high current densities and low turn on voltages. This is due to a more effective injection and transportation of carriers from PEDOT:PSS to PVK as compared to the 3-Et-CVz-PhQ host. Because the HOMO energy (5.5 eV) of TPD is located between that of PEDOT:PSS (5.2 eV) and PVK (5.8 eV), carrier injection and transportation can take place in the PVK:TPD:OXD-7 host system. Among these devices, (3-Et-CVz-PhQ)$_2$Ir(picN-O) is observed to exhibit a better performance than those of (2-Et-CVz-PhQ)$_2$Ir(picN-O) and (btp)$_2$Ir(acac) in solution-processed PhOLEDs. The maximum luminance values of (2-Et-CVz-PhQ)$_2$Ir(picN-O), (3-Et-CVz-PhQ)$_2$Ir(picN-O), and (btp)$_2$Ir(acac) are 618, 9753, and 1016 cd/m^2, respectively. Plots of the external quantum and luminance efficiencies of the Ir(III) complexes as a function of luminance are given in Figure 7. With increasing luminance, the external quantum and luminance efficiencies of (3-Et-CVz-PhQ)$_2$Ir(picN-O) remain stable at 8.74% and 13.86 cd/A at 418 cd/m^2, respectively. Furthermore, the luminance efficiency decreases slightly with increasing current density with only ca. 15% roll-off between 1 and 30 mA/cm^2. This phenomenon indicates that the TCTA interlayer more effectively blocks electrons at the TCTA/EML interface, causing the electrons to be better confined at the interface. Subsequently, the holes and electrons are effectively utilized for recombination as a result of the reduction in the number of holes and electrons passing through the device.[27]

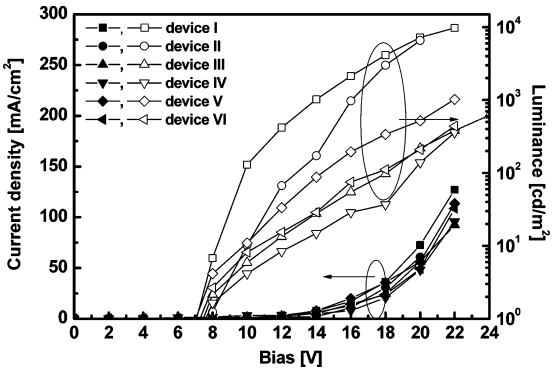

Figure 6. Current density–voltage–luminance (J–V–L) characteristics of (3-Et-CVz-PhQ)$_2$Ir(pic-N-O) and (2-Et-CVz-PhQ)$_2$Ir(pic-N-O).

To understand the structures and orbital properties that are related to electron and hole mobilities, density functional theory (DFT) calculations were performed on (3-Et-CVz-PhQ)$_2$Ir(picN-O) and (2-Et-CVz-PhQ)$_2$Ir(picN-O) by using

dx.doi.org/10.1021/jp2101094 | J. Phys. Chem. C 2012, 116, 7526–7533

Table 2. EL Performance of the Red PhOLEDs Based on a Solution Processed Emitting Layer

emitter	device	host	L_{max} (cd/m^2)	$EQE_{max}^{a,b}$ (%)	$LE_{max}^{a,b}$ (cd/A)	$PE_{max}^{a,b}$ (lm/W)	CIE (x, y)^b
(3-Et-CVz-PhQ)$_2$Ir(pic-N-O)	I	PVK	9753	8.74/7.96	13.86/12.46	4.32/2.44	0.623, 0.374
(3-Et-CVz-PhQ)$_2$Ir(pic-N-O)	II	3-Et-CVz-PhQ	6565	6.08/5.66	10.81/9.78	1.90/1.21	0.624, 0.372
(2-Et-CVz-PhQ)$_2$Ir(pic-N-O)	III	PVK	618	4.32/3.55	0.50/0.39	0.16/0.07	0.680, 0.282
(2-Et-CVz-PhQ)$_2$Ir(pic-N-O)	IV	3-Et-CVz-PhQ	358	1.64/1.35	0.37/0.27	0.05/0.03	0.676, 0.286
Ir(btp)$_2$(acac)	V	PVK	1016	4.58/3.90	1.25/0.94	0.32/0.19	0.678, 0.317
Ir(btp)$_2$(acac)	VI	3-Et-CVz-PhQ	438	1.92/1.55	0.67/0.52	0.16/0.08	0.671, 0.322

^{a}Values recorded at a current density 30 mA/cm^2. ^{b}Values recorded at a current density 20 mA/cm^2.

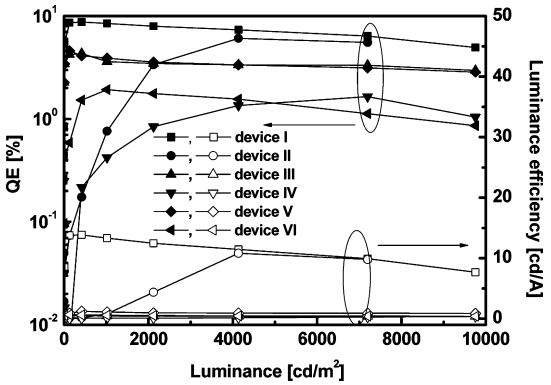

Figure 7. External quantum and luminance efficiencies as a function of luminance for PhOLEDs.

the Becke's three parametrized Lee–Yang–Parr exchange functional (B3LYP) and a suite of Gaussian 03 programs.[28] In a previous study, current calculation methods were shown to reliably predict the structures and electronic properties of similar systems.[19,20] The calculated HOMOs and LUMOs of (3-Et-CVz-PhQ)$_2$Ir(picN-O) and (2-Et-CVz-PhQ)$_2$Ir(picN-O) are shown in Figure 8. It should be noted that no electron population exists in the LUMO of the 3-Et-CVz and 2-Et-CVz moieties after photoexcitation of (3-Et-CVz-PhQ)$_2$Ir(picN-O) and (2-Et-CVz-PhQ)$_2$Ir(picN-O). However, as shown by inspection of the HOMOs, the 3-Et-CVz and 2-Et-CVz moieties have significant electron populations. Thus, the HOMO electrons appear to play a significant role in governing opto-electronic properties, such as absorption and emission. This feature is seen in differences in the energies of the HOMOs, which are −0.173 and −0.163 au for (3-Et-CVz-PhQ)$_2$Ir(picN-O) and (2-Et-CVz-PhQ)$_2$Ir(picN-O), respectively. Importantly, no difference exists in the LUMO energies, which is −0.066 au in both systems. The calculated HOMO–LUMO gaps are 2.919 and 2.646 eV for (3-Et-CVz-PhQ)$_2$Ir(picN-O) and (2-Et-CVz-PhQ)$_2$Ir(picN-O), respectively. These values are in agreement with the experimental observation that devices III and IV display more red-shifted emission (690 nm) than do devices I and II (600 nm). On the basis of the results of the calculations, it is possible to conclude that the emission peak positions of solution processable PhOLEDs can be tuned by HOMO orbital energy differences.

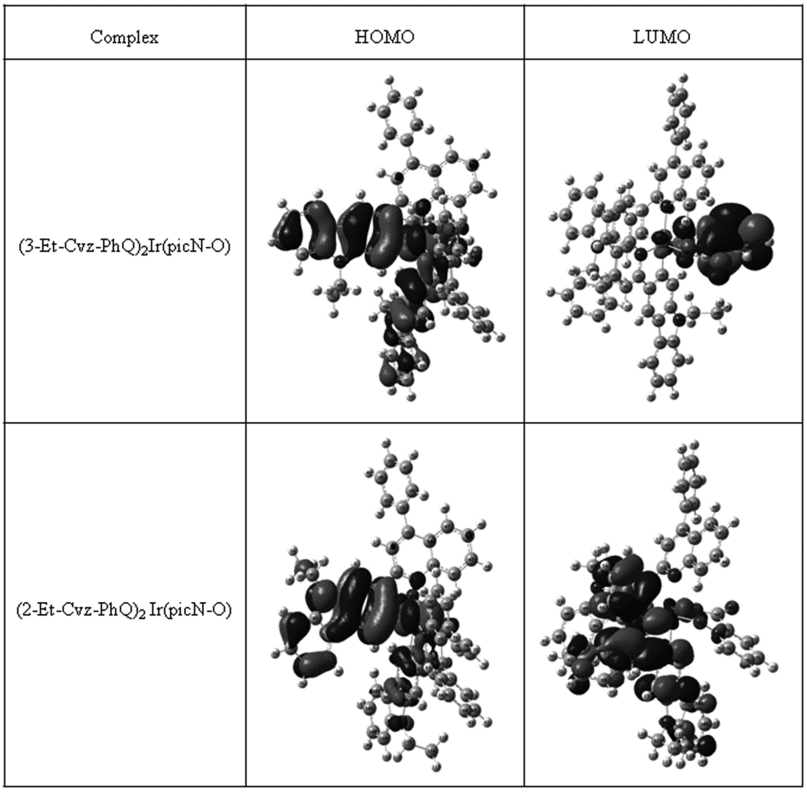

Figure 8. Calculated HOMOs and LUMOs of (3-Et-CVz-PhQ)$_2$Ir(pic-N-O) and (2-Et-CVz-PhQ)$_2$Ir(pic-N-O).

dx.doi.org/10.1021/jp2101094 | J. Phys. Chem. C 2012, 116, 7526–7533

Thus, in general, the emission peak position can be controlled by tuning either HOMO or LUMO orbital energies.

CONCLUSION

As shown by the results presented above, the electro-optical properties of PhOLEDs can be tuned by selection of the positions of ligation of the main ligands to the Ir(III) center. This conclusion derives from studies with $(2\text{-Et-CVz-PhQ})_2$Ir(pic-N-O) and its structural isomer $(3\text{-Et-CVz-PhQ})_2$Ir(pic-N-O), which are coordinated with Ir(III) at the respective C3- and C2-positions of a CVz unit in Et-CVz-PhQ. $(2\text{-Et-CVz-PhQ})_2$Ir(pic-N-O) was observed to display higher thermal stability and a 73 nm greater red-shift than $(3\text{-Et-CVz-PhQ})_2$Ir(pic-N-O). Solution-processed PhOLEDs with $(3\text{-Et-CVz-PhQ})_2$Ir(pic-N-O) or $(2\text{-Et-CVz-PhQ})_2$Ir(pic-N-O) have respective maximum external quantum efficiencies of 8.74% with CIE coordinates of (0.62, 0.37) and 4.32% and deep-red CIE coordinates of (0.68, 0.28). The combination of the performances solution processable PhOLED and color purities makes the materials probed in this effort promising candidates as deep red phosphorescent dopants for PhOLEDs.

AUTHOR INFORMATION

Corresponding Author

*Tel.: +82-51-510-2727. Fax: +82-51-581-2348. E-mail: shjin@pusan.ac.kr (S.-H.J.), jlee@donga.ac.kr (J.W.L.).

Notes

The authors declare no competing financial interest.

ACKNOWLEDGMENTS

This work was supported by the National Research Foundation of Korea (NRF) grant funded from the Ministry of Education, Science and Technology (MEST) of Korea (No. 2011-0028320) and the New & Renewable Energy program of the Korea Institute of Energy Technology Evaluation and Planning (KETEP) grant (No. 20103020010050) funded by the Ministry of Knowledge Economy, Republic of Korea. J.Y.L. acknowledges an NRF grant (No. 20100001630) funded by MEST and a grant from the Fundamental R&D Program for Core Technology of Materials funded by the Ministry of Knowledge and Economy, Republic of Korea.

REFERENCES

(1) Tang, C. W.; Vanslyke, S. A. *Appl. Phys. Lett.* **1987**, *51*, 913.
(2) Wong, W. Y.; Ho, C. L. *J. Mater. Chem.* **2009**, *19*, 4457.
(3) Wong, W. Y.; Ho, C. L. *Coord. Chem. Rev.* **2009**, *253*, 1709.
(4) Tamayo, A. B.; Alleyne, B. D.; Djurovich, P. I.; Tsyba, S. I.; Ho, N. N.; Bau, R.; Thompson, M. E. *J. Am. Chem. Soc.* **2003**, *125*, 7377.
(5) Zhou, G. J.; Wang, Q.; Wang, X.; Ho, C. L.; Wong, W. Y.; Ma, D.; Wang, L.; Lin, Z. *J. Mater. Chem.* **2010**, *20*, 7472.
(6) Wu, H.; Zhou, G.; Zou, J.; Ho, C. L.; Wong, W. Y.; Yang, W.; Peng, J.; Cao, Y. *Adv. Mater.* **2009**, *21*, 4181.
(7) Bera, R. N.; Cumpstey, N.; Burn, P. L.; Samuel, I. D. W. *Adv. Funct. Mater.* **2007**, *17*, 1149.
(8) Adachi, C.; Baldo, M. A.; O'Brien, D. F.; Thompson, M. E.; Forrest, S. R. *J. Appl. Phys.* **2001**, *90*, 5048.
(9) Yang, X. H.; Wu, F. I.; Neher, D.; Chien, C. H.; Shu, C. F. *Chem. Mater.* **2008**, *20*, 1629.
(10) Pu, Y. J.; Higashidate, M.; Nakayama, K. I.; Kido, J. *J. Mater. Chem.* **2008**, *18*, 4183.
(11) Ding, J.; Lü, J.; Cheng, Y.; Xie, Z.; Wang, L.; Jing, X.; Wang, F. *Adv. Funct. Mater.* **2008**, *18*, 2754.
(12) Zhou, G.; Wong, W. Y.; Yao, B.; Xie, Z.; Wang, L. *Angew. Chem., Int. Ed.* **2007**, *46*, 1149.
(13) Wong, W. Y.; Ho, C. L.; Gao, Z. Q.; Mi, B. X.; Chen, C. H.; Chen, K. W.; Lin, Z. *Angew. Chem., Int. Ed.* **2006**, *45*, 7800.
(14) Wang, L.; Gao, Z.; Chen, C. H.; Cheah, K. W.; Lin, Z. *Chem. Asian J.* **2009**, *4*, 89.
(15) Zhang, X.; Chen, Z.; Yang, C.; Li, Z.; Zhang, K.; Yao, H.; Qin, J.; Chen, J.; Cao, Y. *Chem. Phys. Lett.* **2006**, *422*, 386.
(16) Yang, C.; Zhang, X.; You, H.; Zhu, L.; Chen, L.; Z, L.; Tao, Y.; Ma, D.; Shuai, Z.; Qin, J. *Adv. Funct. Mater.* **2007**, *17*, 651.
(17) Ho, C. L.; Wong, W. Y.; Gao, Z. Q.; Chen, C. H.; Cheah, K. W.; et al. *Adv. Funct. Mater.* **2008**, *18*, 319.
(18) Tonzola, C. J.; Kulkarni, A. P.; Gifford, A. P.; Kaminsky, W.; Jenekhe, S. A. *Adv. Funct. Mater.* **2007**, *17*, 863.
(19) Lee, S. J.; Park, J. S.; Yoon, K. J.; Kim, Y. I.; Jin, S. H.; et al. *Adv. Funct. Mater.* **2008**, *18*, 3922.
(20) Lee, S. J.; Park, J. S.; Song, M.; Shin, I. A.; Kim, Y. I.; et al. *Adv. Funct. Mater.* **2009**, *19*, 2205.
(21) Nonoyama, M. *J. Organomet. Chem.* **1975**, *86*, 263.
(22) Agrawal, A. K.; Jenekhe, S. A. *Chem. Mater.* **1992**, *4*, 95.
(23) Rho, H. H.; Park, G. Y.; Ha, Y.; Kim, Y. S. *Jpn. J. Appl. Phys.* **2006**, *45*, 568.
(24) Zhang, X.; Chen, Z.; Yang, C.; Li, Z.; Zhang, K.; Yai, H.; Qin, J.; Chen, J.; Cao, Y. *Chem. Phys. Lett.* **2006**, *422*, 386.
(25) Su, Y.; Huang, H.; Li, C.; Chien, C.; Tao, Y.; Chou, P.; Data, S.; Liu, R. *Adv. Mater.* **2003**, *15*, 884.
(26) Yang, X. H.; Jaiser, F.; Klinger, S.; Neher, D. *Appl. Phys. Lett.* **2006**, *88*, 021107.
(27) Lee, T. W.; Park, O. O.; Yoon, J.; Kim, J. J. *Adv. Mater.* **2001**, *13*, 211.
(28) Frisch, M. J.; Trucks, G. W.; Schlegel, H. B.; Scuseria, G. E.; Robb, M. A.; et al. *Gaussian 03*, revision A1; Gaussian, Inc.: Pittsburgh, PA, 2003.